

Bio-inspired Micromechanical Energy Amplifiers using Variable Stiffness Springs

Yun Jung Heo, Won Chul Lee, and Young-Ho Cho*

Korea Advanced Institute of Science and Technology, Digital Nanolocomotion Center
373-1 Guseong-dong, Yuseong-gu, Daejeon 305-701, Republic of Korea

Abstract

We present a biologically inspired micromechanical energy amplifier using the variable stiffness spring whose stiffness change is proportional to input motion. The present bio-inspired micromechanical energy amplifier modulates the resonant frequency using the variable stiffness spring whose stiffness change is proportional to the input motion, thereby performing the amplification of displacement, force, and energy. The stiffness of the fabricated spring is changed from 9.38N/m to 11.1N/m for the 500Hz input motion varying in the range of 0~0.945 μ m with the 18.5kHz constant carrier motion of 8.06 \pm 0.11 μ m. The displacement, force, and energy gains of 5.62, 7.92, and 44.5 are obtained from the fabricated micromechanical energy amplifier.

Keywords: Micromechanical energy amplifier, Variable stiffness spring, Input-dependent stiffness modulation, Mechanical resonance

1 - INTRODUCTION

The micromechanical amplifiers [1~3] have been developed for high-sensitive microsensors and high-force/long-range microactuators. The previous micromechanical amplifiers using levers [1], membranes [2], or flexible structures [3] are able to amplify only one of displacement or force.

In this paper, we present a biologically inspired micromechanical energy amplifier (Fig.1), which can amplify both displacement and force. Biological inspiration originates from the mechanical energy amplification of outer hair cells in the cochlea: the outer hair cells (Fig.2) amplify the sound-induced input motion by modulating chemical energy of ions using the input-dependent stiffness change of the cell body [4]. The present bio-inspired micromechanical energy amplifier (Fig.1) modulates carrier motion in the mechanical resonance using the variable stiffness spring, thereby performing the amplification of displacement, force, and energy.

2 - WORKING PRINCIPLE

Figure 1 illustrates the working principle of the present micromechanical energy amplifier. First, the input motion is supplied to the variable stiffness spring, while the carrier motion in the mechanical resonance is transmitted to the amplifier. When the input motion is supplied to the variable stiffness spring, the output stiffness of the variable stiffness spring alters. The stiffness change causes the resonant frequency shift of the amplifier. The amplitude of the carrier motion in the carrier frequency of f_c is decreased due to the resonant frequency shift, as shown in Fig.3. Finally, the

amplifier generates the output motion resulted from the amplitude change of the carrier motion according to the input motion. Envelope of the output motion contains the amplified input motion.

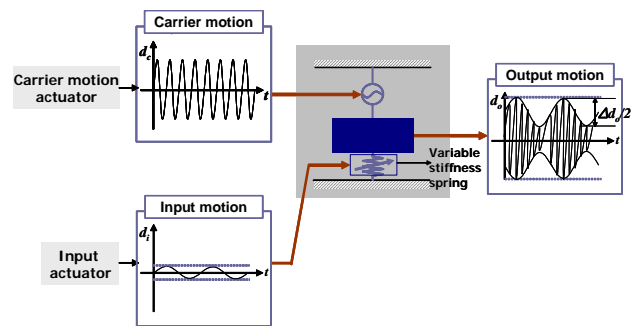


Figure 1 – Simplified model of the micromechanical energy amplifier

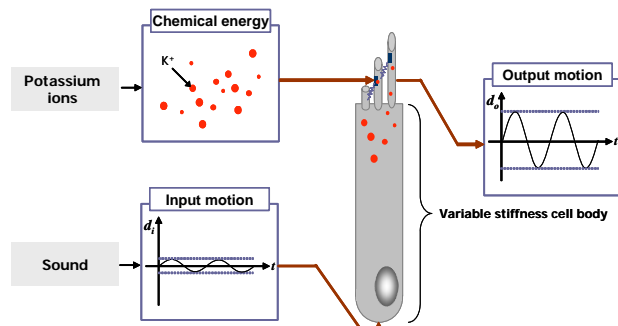


Figure 2 – Simplified model of the hair-cell energy amplifier.

* Contact author: Tel. +82-42-869-8691, Fax: +82-42-869-8690, email: nanosys@kaist.ac.kr

Figure 4 illustrates the micromechanical energy amplifier, composed of the variable stiffness spring and the carrier motion actuator. The variable stiffness spring is designed to change its output stiffness depending on the input motion. The carrier motion actuator generates the carrier motion in the mechanical resonance. In order to supply input motion to the amplifier, we attach the input actuator to the input port of the variable stiffness spring, as shown in Fig.5.

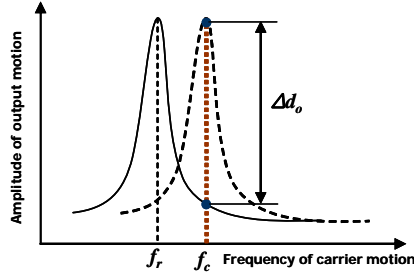


Figure 3 – Amplified output motion due to the resonant frequency shift from f_c to f_r : the resonant frequency shift is caused by the spring stiffness spring (Fig.5) depending on the input motion.

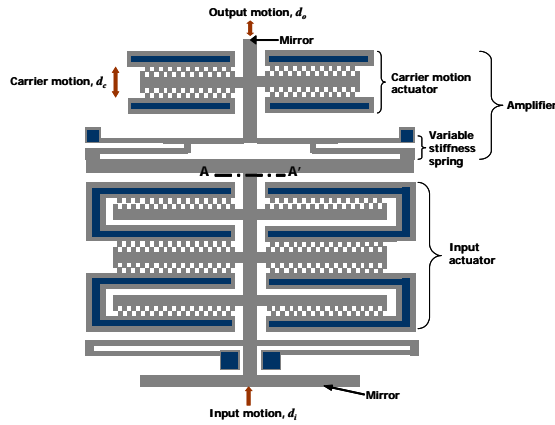


Figure 4 – Top view of the micromechanical energy amplifier.

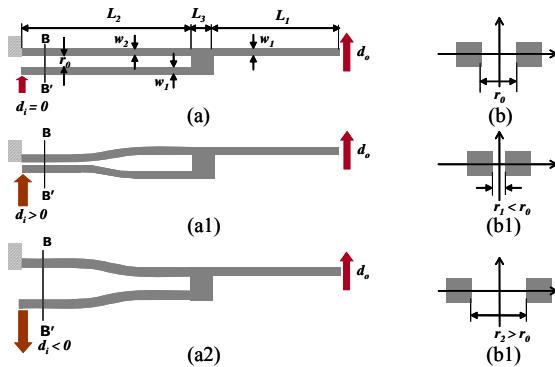


Figure 5 – Structure and principle of the variable stiffness spring: (a) and (b) illustrate the spring and its cross section of BB' at the initial input condition of $d_i=0$; (a1) and (b1) showing the spring stiffness reduction at the input condition of $d_i>0$; (a2) and (b2) showing the spring stiffness increase at the input condition of $d_i<0$.

Table 1 – Dimension and property of the variable stiffness spring, as shown in Fig.5(a).

Spring dimension and property	Values
Beam lengths (L_1, L_2, L_3)	174 μm , 347 μm , 20 μm
Beam width (w)	3.2 μm
Initial gap between beam (r_0)	3.8 μm
Initial gap between beams (r_0)	7.05 N/m
Output stiffness (k_o at $d_i=0$)	9.38 N/m

Table 2 – Input-dependent spring stiffness and amplifier frequency for the carrier motion input of 8.06 μm at 18.5 kHz

	Variation	Variation/ d_i
Input motion (d_i) at 500 Hz	0~0.945 μm	1
Input stiffness (k_i)	7.05 N/m	0
Output stiffness (k_o)	9.38~11.1N/m	1.82 N/m/ μm
Amplifier freq. (f_r)	17.4~18.9 kHz	1.59 kHz/ μm

Figure 5 illustrates the structure and principle of the variable stiffness spring. The input motion changes the initial gap, r_0 , between two beams and changes the second area moment of the variable stiffness spring, thus modifying the output stiffness of the variable stiffness spring. For the variable stiffness spring of Fig.5, the output stiffness, k_o , is varying proportional to the input motion and the input stiffness, k_i , is at a constant value. Table 1 lists the dimension and properties of the variable stiffness spring of Fig.5.

3 - MICROFABRICATION

Figure 6 illustrates the single-mask SOI fabrication process for the cross section along A-A' in Fig.4. The prototypes are made by a top silicon layer of SOI (Silicon On Insulator) wafer in Fig.6a. In Fig.6b, the prototypes are defined by the silicon deep RIE etching of the 20 μm -thick single crystal silicon. In Fig.6c, a 2 μm -thick buried oxide layer is removed by using BOE (Buffered Oxide Etchant) solution. The wafer, rinsed in isopropyl alcohol, is dried in an infrared lamp. In Fig.6d, 200 \AA /2300 \AA -thick Cr/Au layers are sputtered to form electro pads for gold wire bonding. Figure 7 shows SEM photographs of the overall structure and the amplifier parts of the fabricated devices.

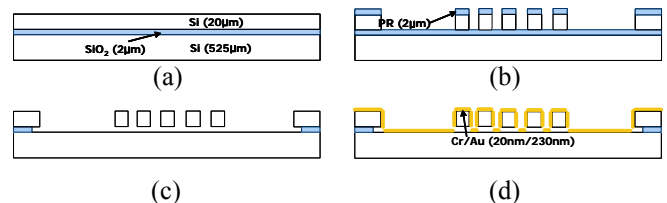


Figure 6 – Fabrication process for the cross section along A-A' in Fig.4.

4 - EXPERIMENTAL RESULTS

We analyze the micromechanical energy amplifier by measurement of the stiffness modulation and the amplification performance. The input actuator is driven by 500Hz sine waves, while the carrier motion actuator is driven by an 18.5kHz sine wave. The input and output motions of the present device are measured through mirrors which are attached at the end of the input actuator and the carrier motion actuator, respectively. We use a laser interferometer, LDV (Laser Doppler Vibrometer) to measure the mirror motions.

4.1 - The stiffness modulation

Figure 8 shows the estimated and measured relative stiffness change of the variable stiffness spring for the input motion. Table 2 summarizes the stiffness modulation of the variable stiffness spring and the resonant frequency shift of the amplifier due to the input motion. We obtain the output stiffness modulation in the variable stiffness spring of 1.82N/m/ μm for varying input motions in the range of 0~0.945 μm . We measure the dynamic characteristics of the amplifier, and then we attain the resonant frequencies of the amplifier for the input motion. The amplifier shows the resonant frequency shift of 1.59kHz/ μm for varying input motions in the range of 0~0.945 μm .

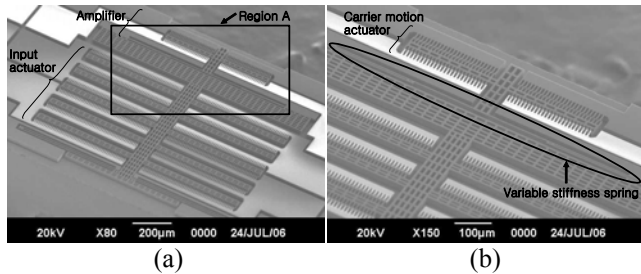


Figure 7 – SEM photographs of the micromechanical energy amplifier: (a) overall structure; (b) an enlarged view of the Region A in (a).

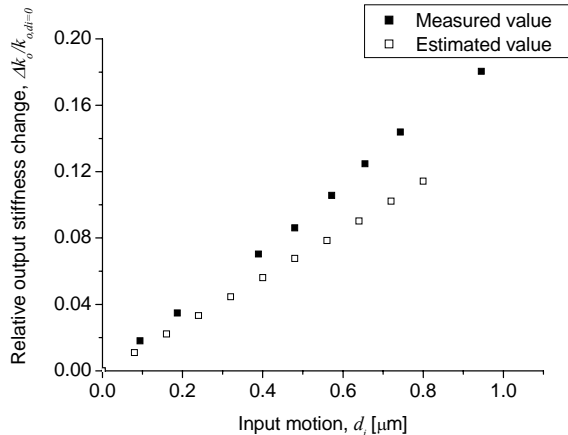


Figure 8 – Estimated and measured relative stiffness change of the variable stiffness spring for varying input motion.

Table 3 – Measured performance of the micromechanical energy amplifier

	Input	Output	Gain
Motion	0~0.945 μm	0~5.07 μm	5.62
Force	0~ 7.01×10^{-6} N	0~ 5.62×10^{-5} N	7.92
Energy	0~ 3.19×10^{-12} J	0~ 1.42×10^{-10} J	44.5

4.2 - The amplification performance

Figure 9 shows measured input and output motions of the amplifier and the amplitude change of the output motion for varying input motions in the range of 0~0.945 μm . The output motion forms a 500Hz sine wave such as the input motion. The envelope of the output motion has larger amplitude than the amplitude of the input motion, as shown in Fig.9a. We obtain the displacement gain of 5.62 from the inclination of the detected signals in Fig.9b. The force gain, G_F , is given by,

$$G_F = \frac{k_o \Delta d_o}{k_i d_i} \quad (1)$$

The force gain of the amplifier is proportional to the output to input stiffness ratio, k_o/k_i , and the displacement gain, $\Delta d_o/d_i$. The energy gain, G_E , is given by,

$$G_E = \frac{k_o \Delta d_o^2}{k_i d_i^2} \quad (2)$$

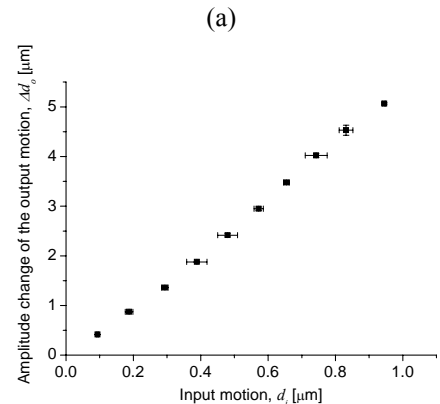
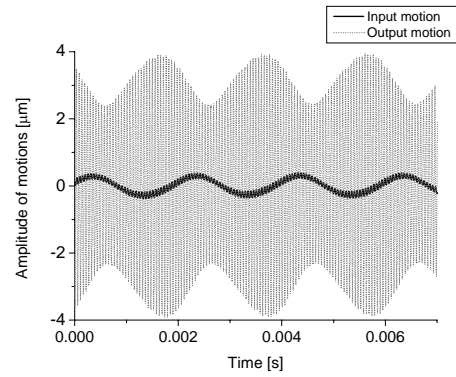


Figure 9 – Estimated and measured relative stiffness change of the variable stiffness spring for varying input motion.

The energy gain is proportional to the output to input stiffness ratio, k_o/k_i , and the square root of displacement gain, $\Delta d_o/d_i$. The displacement, force and energy gains of the amplifier are obtained by 5.62, 7.92, and 44.5, respectively, as summarized in Table 3.

5 - CONCLUSIONS

In this paper, we presented the micromechanical energy amplifier using the carrier motion in the mechanical resonance modulated by the variable stiffness spring depending on the input motion. In the experimental study, we fabricated the micromechanical energy amplifier and measured the stiffness modulation of the variable stiffness spring and the amplification performance of the amplifier. We obtained the stiffness modulation in the variable stiffness spring of the 1.82N/m/ μm . The displacement, force, and energy gains of the amplifier are characterized as 5.62, 7.92, and 44.5, respectively. On these experimental bases, we can conclude that the present bio-inspired micromechanical amplifier is able to amplify displacement, force, and energy, suitable for high-sensitive sensing and high-force actuation devices.

ACKNOWLEDGMENTS

This work has been supported by the National Creative Research Initiative Program of the Ministry of Science and Technology (MOST) under the project title of "Realization of Bio-Inspired Digital Nanoactuators."

REFERENCES

- [1] M. Aikele, K. Bauer, W. Ficker, F. Neubauer, U. Prechtel, J. Schalk, and H. Seidel, "Resonant Accelerometer with Self-test," *Sensors and Actuators A*, Vol. 92 (2001), pp. 161-167.
- [2] T.G. Kang, K.-S. Seo, Y.-H. Cho, O H. Baek, W. L. Hwang, and J. H. Moon, "A Long-Stroke Thermopneumatic Actuator for Applications to Microflow and Pressure Regulation," *Proc. Inter. Conference on New actuators (Actuator '98)*, Bremen, Germany, June, 1998, pp.62-65.
- [3] S. Kota, J. Hetrick, Z. Li, S. Rodgers, and T. Krygowski, "Synthesizing High-performance Compliant Stroke Amplification Systems for MEMS," *Proc. 13th IEEE Inter. Conf. on Micro Electro Mechanical Systems (MEMS-2000)*, Miyazaki, Japan, January, 2000, pp.164-169.
- [4] P. Dallos, A. N. Popper, and R. R. Fay, Outer Hair Cell Motility in *The Cochlea*, Springer-Verlag, New York, 1996, Chap.7.